Proceedings of the Korean Nuclear Society Autumn Meeting
Yongpyong, Korea, 2003

A Study of Downcomer Boiling during Reflood Phase using TRAC-M Code

Woochong Chon, Jae-Hoon Lee, Byung Sok Kim, Sang-Jong Lee and Chang-Sok Cho

Kepco Nuclear Fuel Co. ltd
493 Deokjin-dong, Yuseong-gu
Daejeon, KOREA 305-353

Abstract

The capability of TRAC-M code to predict downcomer boiling effect during reflood phase in postulated PWR LOCA is evaluated using the results of downcomer effective water head experiment and Cylindrical Core Test Facility (CCTF) C1-2 (Run 11)/C1-3 (Run 12) experiments, which were performed at JAERI in 1977 and 1979. With a full height downcomer simulator, effective water head experiment was carried out under 1 atm to investigate the applicability of the correlation for void fraction to evaluate the effective water head in downcomer. In order to clarify the effect of the initial superheat of the downcomer wall on the system and the core cooling behaviors during the reflood phase of a PWR LOCA, two tests were also performed with a CCTF. C1-2 test is the superheated downcomer wall test with the initial superheat of 79 K, as in the actual PWR, and C1-3 is the saturated downcomer wall test without initial superheat.

Results show that TRAC-M code tends to under-predict downcomer effective water head and core differential pressure. And the code results show a good agreement with the experimental results in downcomer temperature, heat flux and pressure. Code predicted core cladding temperature and quench time are still higher than the measured experimental results in CCTF tests. Both experiment and calculation data show the lower downcomer water head with the initial superheat of the downcomer wall test. But the difference of the core inlet mass flow rate was small between the superheated and the saturated wall tests.

1. Introduction

Downcomer boiling is caused by metal heat release from vessel and core barrels walls to fluid in the downcomer gap. Metal heat from the vessel lower head and structures in the lower plenum also contribute to downcomer boiling. As heat is released to the downcomer fluid, its temperature is gradually increased and eventually subcooled and saturated boiling takes place. Voids generated by these processes displace water in the downcomer and reduce the water head which is the only driving force to supply emergency core coolant into core during reflood phase in a large cold leg break loss of coolant accident (LOCA). This loss in driving force can significantly reduce the core flooding rate. Hence, it is necessary to understand clearly the physical phenomenon of downcomer boiling during reflood phase.

Evaluation Models based on Appendix K do not necessarily capture this phenomenon, since nodalization of the downcomer and modeling of subcooled boiling is simplified in those types of Evaluation Models. This prohibits the code from calculating thermal stratification for the entire vessel component. Previous experimental and numerical studies have shown that neglecting downcomer boiling during reflood in a large break loss-of-coolant accident could be a non-conservative assumption.

The effect of the superheated wall on the downcomer water head was studied by Sudo, et al. [1] with the test facility modeling the downcomer part of the actual PWR system. They confirmed experimentally that the static water head was decreased because of the steam generation due to the heat release from the superheated slab. They developed a correlation to evaluate the void fraction in the downcomer and studied the effect of the scaling factor and the applicability of the correlation for the prediction of the static water head. The effect of the initial superheat of the downcomer wall on the system behavior was studied by Akimoto and Murao using the Cylindrical Core Test Facility [2]. They concluded that the initial superheat of the downcomer wall resulted in the lower downcomer water head and caused the core inlet subcooling to be decreased, and led to the lower core water head. But they showed the difference of the core inlet mass flow rate was small between the superheated and the saturated wall tests since the compensation of the decresed mass flow rate through the intact loops by the increase mass flow rate through the broken loop.

The purpose of this study is to investigate the capability of TRAC-M code to predict downcomer boiling effect during reflood phase in postulated PWR LOCA [3]. The first downcomer simulation model is composed of two flat plates located in parallel to simulate the rectangular downcomer flow channel and has three regions simulating a lower plenum, effective heated region and upper annulus. Two different geometries, Cylindrical and Cartesian, are applied in simplified downcomer simulation model. And also sensitivity study for different nodalization was done. The second applied model is CCTF Core 1 which is an experimental facility designed to model Westinghouse 4-loop PWRs. It is a full-height test facility built and operated by JAERI. Cylindrical coordinate system is used in CCTF model and calculations are done for both superheated and saturated downcomer wall tests.

2. Description of Works

2.1 Downcomer Effective Water Head Test Description

A schematic view of test facility is shown in Fig. 1 [1]. Test facility is composed of a downcomer simulator, water supply system, vent lines for steam and water, water extraction line and measurement system. The downcomer simulator is made of two carbon steel flat plates located in parallel to make up the rectangular downcomer flow channel, whose dimension is 6.5 m in height, 1 m in width and 0.2 m in gap. The gap of flow channel is changeable from 0.05 to 0.2 m by inserting box-type internals into the flow channel in order to investigate the effect of the gap on the effective water head. But fixed 0.2 m gap test is chosen for current study. The downcomer simulator is composed of three regions simulating a lower plenum, effective heated region and upper annulus. The lower plenum region is unheated and 0.5 m in height. The upper annulus region is also unheated and 1.0 m in height. The effective heated region is 5.0 m in height and heaters are attached on the outer surfaces in the effective heated region in order to heat the walls up to 300 ^{o}C.

Actual downcomer walls of a typical PWR have stainless steel cladding on the inner surfaces. Therefore, cladding is required to properly simulate histories of heat release from

walls into fluid and besides, prevents the erosion of carbon steel by water during tests. The dimensions of two flat plates are 6.5 m in height, 1.0 m in width, 0.05m in thickness of carbon steel plate and 0.006 m in thickness of stainless steel cladding. In order to inject emergency core coolant, two water supply lines are provided to the downcomer simulator. One is an initial injection line and the other is a low pressure coolant injection (LPCI) line. The initial injection line is used to establish two phase mixture over the downcomer flow channel as fast as possible by injecting water with a high flow rate at the bottom of the downcomer. On the other hand, LPCI line is used to simulate the cold leg injection by injecting water at the top of the effective heated region of the downcomer. A water overflow line is provided at the top of the effective heated region of the downcomer. In case of current test, the velocity of injected water through the initial injection line at the lower plenum is 0.2 m/s for initial 30 sec and 0.035 m/s from the LPCI line after that.

As for the instruments, 25 sets of thermocouples and 11 differential pressure transducers are equipped at different elevations of downcomer walls. A set of thermocouples is composed of three thermocouples, which are located at 0, 8 and 51 mm apart from the inner surface in the wall at each elevation.

2.2 CCTF C1-2 Test Description

The CCTF was designed to reasonably simulate the flow conditions in the primary system of a four loop PWR during the refill and reflood phases of a LOCA [2]. The reference reactors are the Trojan reactor and, in certain aspects, the Ohi reactor in Japan. The vertical dimensions and the flow paths of the system components in the CCTF are kept as close to the reference reactor as possible. The flow area of each system component is scaled down in proportion to the scaling factor of the core flow area, that is, 1/21.4. The assumed break location is the cold leg piping corresponding to the outer surface of the biological shield of the reference reactor.

The CCTF facility is equipped with four primary loops, which are composed of three intact loops and a broken loop. Each loop has a hot-leg-piping section, an active steam generator, a loop-seal-piping section, a pump simulator, an emergency core cooling (ECC) injection port and a cold-leg-piping section. The emergency core cooling system (ECCS) of the CCTF consists of the accumulator (ACC) and LPCI systems. Each system is connected to the ECC water injection ports attached at the cold legs and the lower plenum of the pressure vessel.

The core consists of 32 bundles arranged in a cylindrical configuration. Each bundle consists of 8x8 heater rods and it contains 57 heater rods and 7 non-heated rods. The 57 heater rods consist of 12 high, 17 medium and 28 low power rods. The power ratios of the high, medium and low power rods to the bundle-average power are 1.1, 1.0 and 0.95, respectively.

The design of the upper plenum internals is based on that for the Westinghouse 17x17 array fuel assemblies. The radial dimension of each internal is scaled down by factor of 8/15 from that of the reference reactor because the heater rods of the CCTF simulate the 15x15 array fuel assembly. The CCTF has 12 control rod guide tubes, 4 support columns, 8 stub mixers, 2 orifice plates and 6 open holes in upper plenum internals.

The downcomer is an annulus with 0.0615 m gap in the CCTF. In the scaling of the CCTF downcomer, the volume of the baffle region in the reference reactor was added to the volume of the downcomer. The CCTF has a wider downcomer gap. However, the wider downcomer provides more conservatisms in the downcomer water accumulation rate. The outside wall of the downcomer is constructed of carbon steel cladded with 0.005 m stainless steel. The

thickness of carbon steel is 0.085 m. The wall is preheated to a certain temperature before the test.

2.3 TRAC Modeling for Downcomer Effective Water Head Test

To simulate current test, TRAC-M F90 Ver. 3.782 code has been used [3]. This test loop is modeled using 9 components including 2 heat structures, and 6 juncions. The downcomer simulator is modeled as vessel component without reactor-core region in 3D Cartesian coordinate as shown in Fig 2. The 12 axial cells are set with considering the position of temperature censers installed on the downcomer simulator plates. One ACC inlet pipe is connected with level 1 and other LPCI inlet pipe and overflow outlet pipe are connected with level 12. The total cell number is 2 in X-direction and 1 in Y-direction. Injection time is controlled by TRIP and time based mass flow rate table given in FILL components to set the same boundary conditions with experiment. The initial pressure is set on 1 atm. The Blasius interfacial drag correlation is applied in the lower plenum and downcomer of VESSEL component. In addition, cylindrical coordinate is tested for comparison. The calculation is also performed with the axial cell number change to 19 and 31 for the evaluation of node sensitivity. Test conditions and dimensions used for calculation input are the same as experimental conditions and main test conditions are given in Table 1.

Table 1. Test Conditions for Downcomer Water Head Test

Test Condition	Input
System Pressure (Pa)	1.0E+05
Downcomer Wall Temp. (K)	523
ECC Liquid Temp. (K)	372
Initial Injection Rate (m/s)	0.2
LPCI Rate (m/s)	0.035

2.4 TRAC Modeling for CCTF Test

The CCTF test loop is modeled using 53 components, 31 junctions and 24 heat structures. In TRAC code, the pressure vessel is modeled in 3D cylindrical coordinate as shown in Fig. 3. The pressure vessel is divided into 22 axial levels, four radial rings and four azimuthal sectors for a total of 352 fluid cells for nodalization. The fourth ring from the core center simulates downcomer area. The lower plenum nodding contains three axial levels. For the code to adequately model the sweepout effect, analysis has shown that at least two cells are required below the downcomer skirt. The upper plenum is defined as the region between the top of the active core and the bottom of the upper head. From the outlet of the active core to the nozzle region, four cells are defined. Level 22 represents upper head area. The hot and cold legs are connected to level 20. The heater rods are located from level 4 to level 15 and total length is 3.66 m. ACC and LPCI injection times are controlled by flow rate tables given in FILL components to set the same conditions with experiment. The main test conditions are given in Table 2.

All four loops are modeled identically except loop 4 contains the cold leg break between the pump simulator and reactor vessel. Each loop models the hot leg piping, steam generator primary and secondary fluid volume and heat transfer. Each loop also contains modeling of the accumulator and high and low pressure injection ECCSs. The hot leg connects the reactor vessel to the steam generator inlet plenum. The hot leg is modeled with a TEE component to allow for the connection of the pressurizer surge line. The primary tube of the TEE is modeled identically to the PIPE components in the other loops. The U-tubes are modeled for the boiling region of the steam generator. The dominant phenomena to capture are steady state heat balance and steam binding during reflood. The pump discharge cold leg region is modeled with a TEE component. The secondary tube of the TEE provides for ECC injection.

The core consists of three radial rings, which have different power ratios of the high, medium and low power RODs. The average powers are 1.158, 1.080 and 0.885, respectively. The time dependent ROD power decay is given by table in ROD component, which is obtained from experiment data.

Table 2. Test Conditions for CCTF C1-2 and C1-3 Tests

Test Conditions	C1-2	C1-3
Total Power (MW)	9.36	9.35
Linear Power (KW/m)	1.40	1.40
Radial Power Distribution	1.158:1.080:0.885	1.158:1.080:0.885
System Pressure (MPa)	0.211	0.208
Containment Pressure (MPa)	0.2	0.2
Initial Downcomer Wall Temp. (K)	460	388
Vessel Internals Temp. (K)	393	383
Primary Piping Walls Temp. (K)	391	383
Lower Plenum Liquid Temp. (K)	386	379
ECC Liquid Temp. (K)	312	311
SG Secondary Side Temp. (K)	536	537
PCT at ECC Initiation (K)	775	775
Accumulator Flow Rate (m^3/s)	0.0672	0.07
LPCI Flow Rate (m^3/s)	0.00858	0.008556
Initial Water Level in Lower Plenum (m)	0.86	0.85

3. Results

3.1 Downcomer Effective Water Head Test

Figure 4 shows the comparison of wall temperature histories between experiment and calculation at the 0.85 m height from the bottom of heated region. Three different distances

of 0, 8 and 51 mm from the inner surface of downcomer simulator plate are set for the temperature measurement at the same elevation. The temperature trends of calculation result are very similar to experimental result. The temperature differences are shown especially at the water injection period since water level is not exactly flat during the water injection in experiment. And other temperature differences inside wall seems due to the different effect of conduction during measuring process using thermocouples in experiment. Figure 5 shows the comparison of wall temperature histories at the 4.15 m height from the bottom of heated region. It also shows good matches except at the period of water injection started since the injection starting time not exactly same as experiment. The temperature differences at the beginning of experiment are shown since steady state condition was not achieved during temperature measurement.

Figure 6 shows the comparison of pressure difference between experiment and calculation at the elevation 0 ~ 0.685 m from the bottom of heated section. TRAC result shows oscillation during the calculation but average pressure difference is lower than that of experimental result. It shows the trend of pressure difference is similar with experimental result but bigger oscillation is occurred during the calculation. The TRAC calculation results tend to under-predict downcomer water head at various elevations. Figure 7 shows the comparison of heat flux calculated from temperature history of experimental result with data calculated. It shows that most of data points are located within 20 % error range. Figure 8 shows the comparison of temperature history between Cartesian coordinate and Cylindrical coordinate calculation. It shows the same result for both coordinate systems. Figure 9 shows the comparison of temperature history with different axial cell numbers of 12 and 19. It also shows that calculation is not varying with different axial cell numbers.

3.2 CCTF Test

Figure 10 shows the comparison of the clad surface temperature histories between experiment and calculation. The temperatures of experimental data were measured from two different elevations of 2.44 m and 3.995 m from the bottom of heated section along an average power rod. TRAC data shown in this figure is maximum temperature of average power rod. It shows that the turnaround time and temperature at the same elevation are nearly the same between C1-2 and C1-3 tests in both results. Whereas the quench time in the superheated wall test is longer than that of the saturated wall test. The effect of the initial superheat of the downcomer wall on the core cooling becomes significant in the later period of the reflood phase. The TRAC results show over-predict clad surface temperatures compare with experiment and temperature history trends are the same.

Figure 11 shows the comparisons of differential pressures between the bottom and the top of the downcomer, that is, the downcomer water head. The friction loss is negligibly small comparing to the static water head in the downcomer since the water and the steam velocities are relatively small in the downcomer. The TRAC results show that the pressure differences about 80 sec after starting calculation has large oscillation since condensation is occurred after LPCI injection started. Result also shows that calculation data over-predict untill about 180 sec after test started and under-predict after that. The differential pressure of superheated downcomer wall temperature test (C1-2) data shows lower level than saturated wall temperature from 120 sec after test started.

Figure 12 shows the comparison of differential pressure in the core. It shows calculation data has large oscillation and under-predict over test period compare with experimental data, but trends are similar to experimental data. It shows superheated downcomer wall temperature test result has relatively lower core differential pressure, but difference is small.

Figure 13 shows the comparison of the integration of core inlet mass flow between both tests. The mass flow rate of experimental result was evaluated by the mass balance calculation for the pressure vessel. The error of the evaluated core inlet mass flow rate was estimated to be about 15% at most. The difference of the core inlet mass flow rate between superheated wall and saturated wall tests is small in both experiment and calculation. TRAC results shows less amount of water mass is collected after 220 sec in both cases. But they are in the range of the estimation error of the core inlet mass flow.

4. Conclusions

From the present study, the following conclusions were obtained:

Downcomer Boiling effect can be analyzed by using the TRAC-M code and the present modeling scheme.

From the downcomer effective water head test, the inner wall surface temperature shows rapid decrease just after the mixture level reaches the certain point and after that the temperature decreases slowly to the saturation temperature. TRAC calculation heat flux results show good agreement and are within 20 % difference range compare with experimental results.

The CCTF test results show that TRAC-M code tends to under-predict downcomer effective water head and core differential pressure. And the code results show a good agreement with the experimental results in cladding surface temperature, and downcomer pressure. Code predicted core cladding temperature and quenching time are still higher than the measured experimental data in CCTF tests. Both experiment and calculation data show the lower downcomer water head with the initial superheat of the downcomer wall test. But the difference of the core inlet mass flow rate was small between the superheated and the saturated wall tests.

References

1 Yukio SUDO and Hajime AKIMOTO, 1982, Downcomer Effective Water Head during Reflood in Postulated PWR LOCA, *Journal of Nuclear Science and Technology*, 19[1], pp. 34~45.

2 Hajime AKIMOTO, and Yoshio MURAO, 1983, Evaluation Report on CCTF Core-1 Reflood Test C1-2 (Run 11) and C1-3 (Run 12), JAERI-M 83-090.

3 R. G. Steinke et al., “TRAC-M/FORTRAN 90 (Version 3.0) User’s Mannual,” NUREG/CR-6722, Los Alamos National Laboratory, May 2001

4 Yukio SUDO and Yoshio MURAO, 1978, Experiment of the Downcomer Effective Water Head during a Reflood Phase of PWR LOCA, JAERI-M 7978.

5 Yukio SUDO and Yoshio MURAO, 1978, Preliminary Analysis of Downcomer Effective Water Head during Reflood Phase in PWR LOCA, JAERI-M 7490

6 Yukio SUDO, Yoshio MURAO, and Hajime AKIMOTO, 1980, Experimental Results of the Effective Water Head in Downcomer during Reflood Phase of a PWR LOCA, JAERI-M 8978.

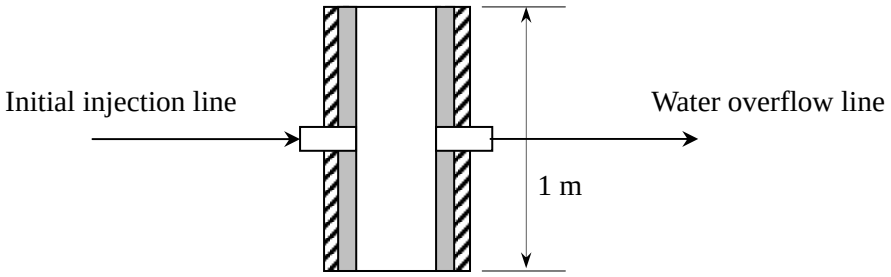

(a) Top View

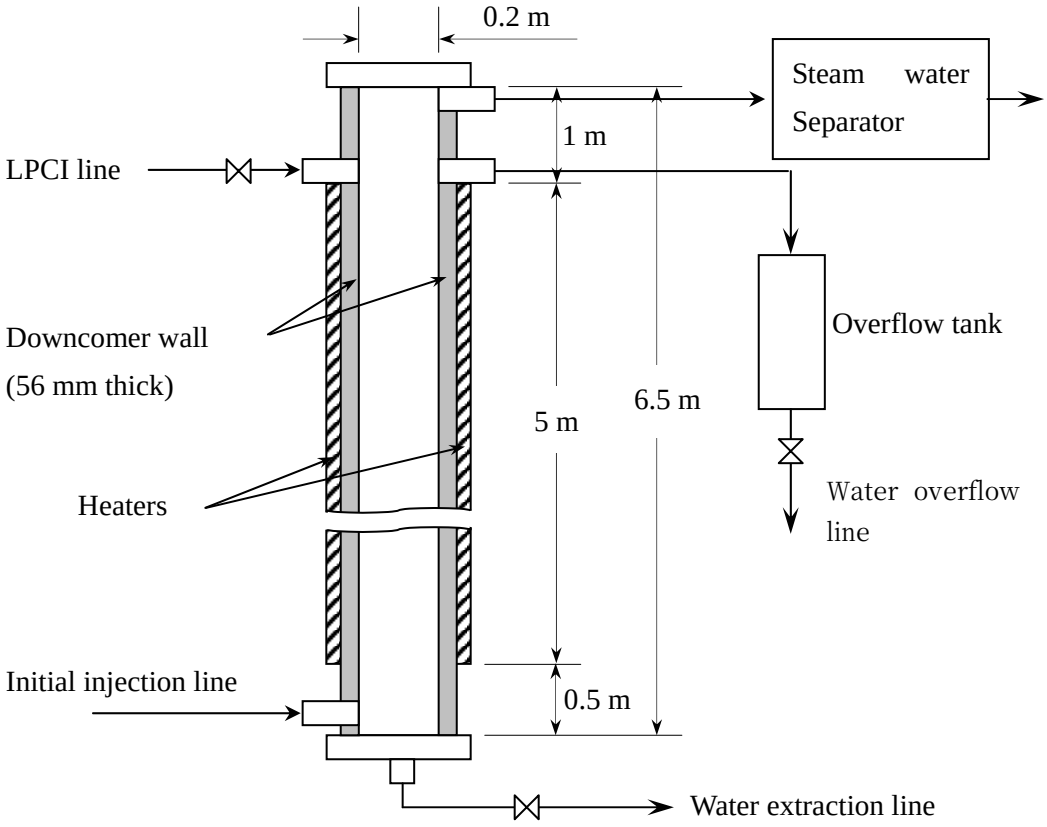

(b) Side View

Figure 1. Schematic View of Effective Downcomer Water Head Experiment Facility

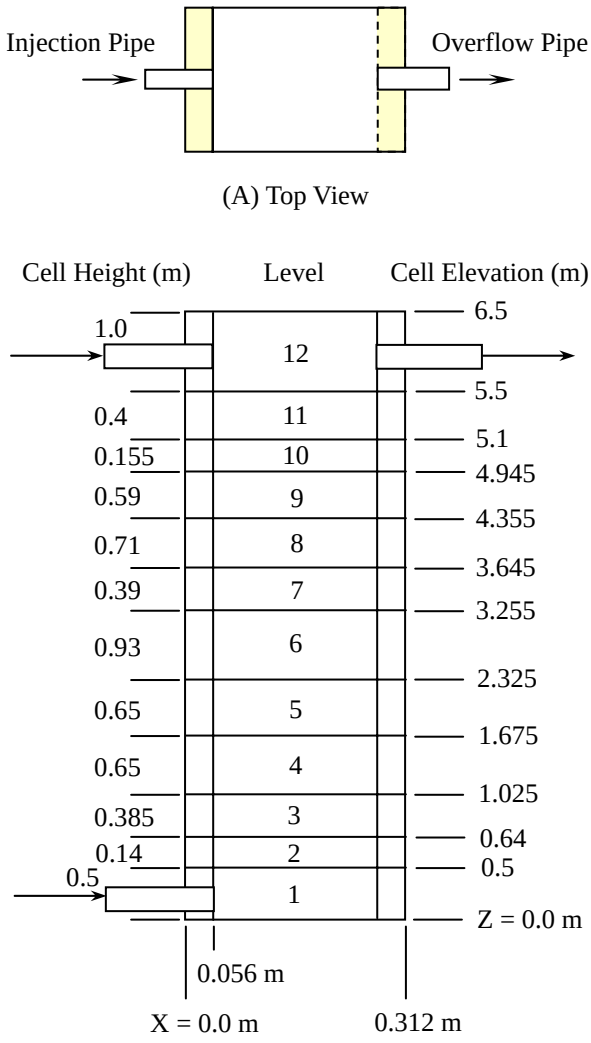

Figure 2. Vessel Nodalization for Effective Downcomer Water Head Test

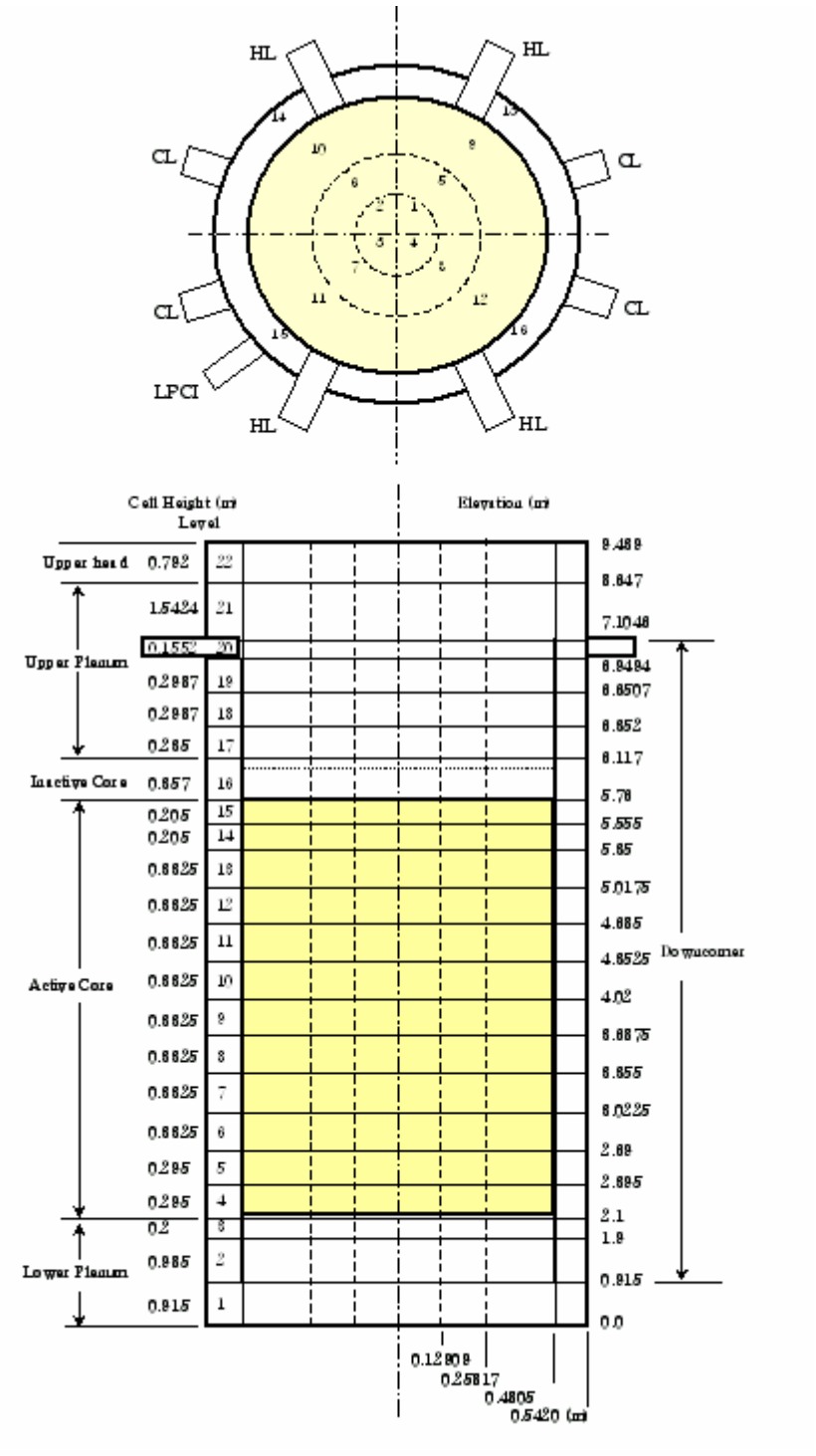

Figure 3. Vessel Nodalization for CCTF Test

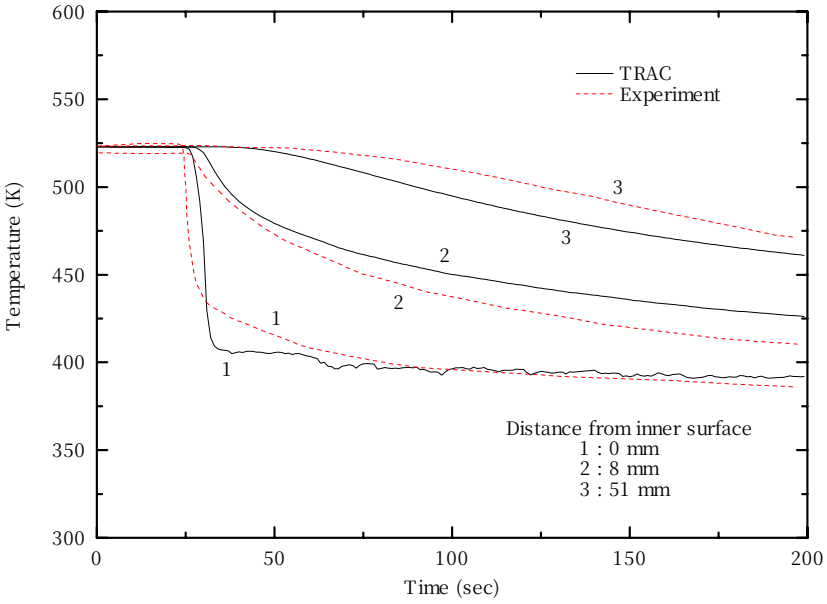

Figure 4 Comparisons of Temperature Histories between Experiment and Calculation
(Hight from the Bottom of Heated Region : 0.85 m)

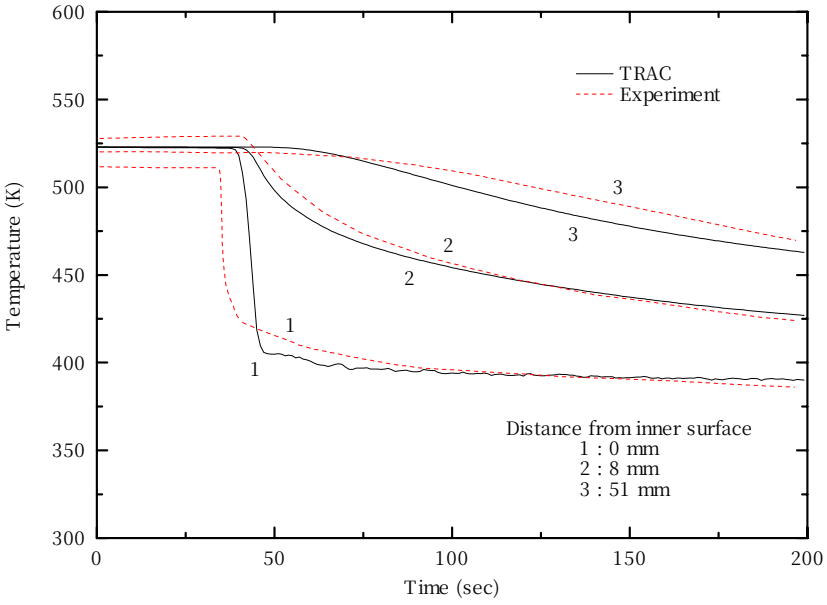

Figure 5 Comparisons of Temperature Histories between Experiment and Calculation
(Hight from the Bottom of Heated Region : 4.15 m)

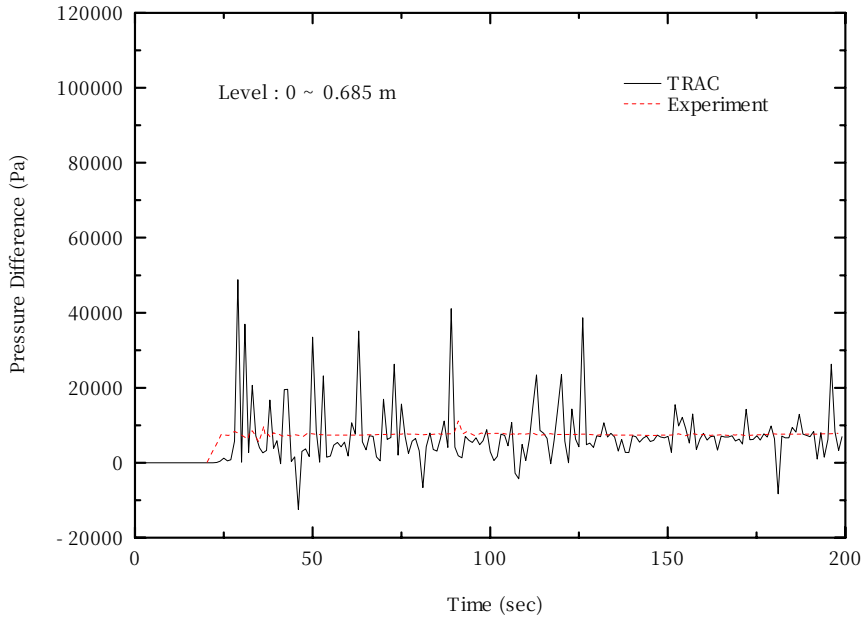

Figure 6. Comparison of Differential Pressure between Experiment and Calculation (0 ~ 0.685 m)

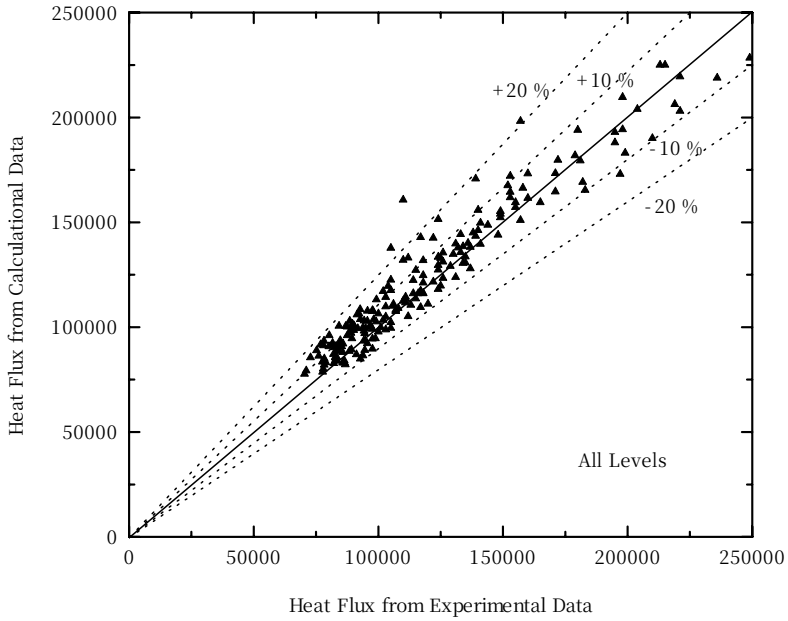

Figure 7. Comparison of Heat Flux between Experiment and Calculation

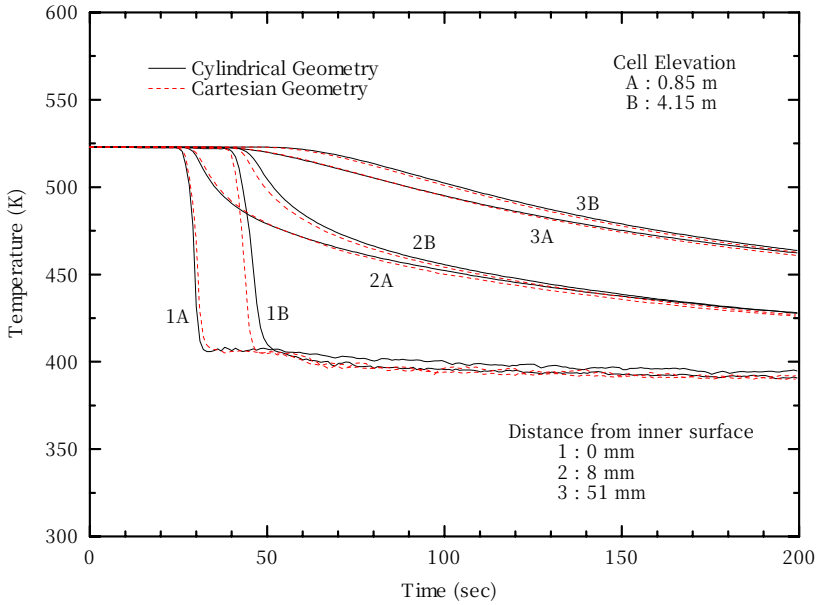

Figure 8 Comparisons of Temperature Histories between Cylindrical and Cartesian Coordinate

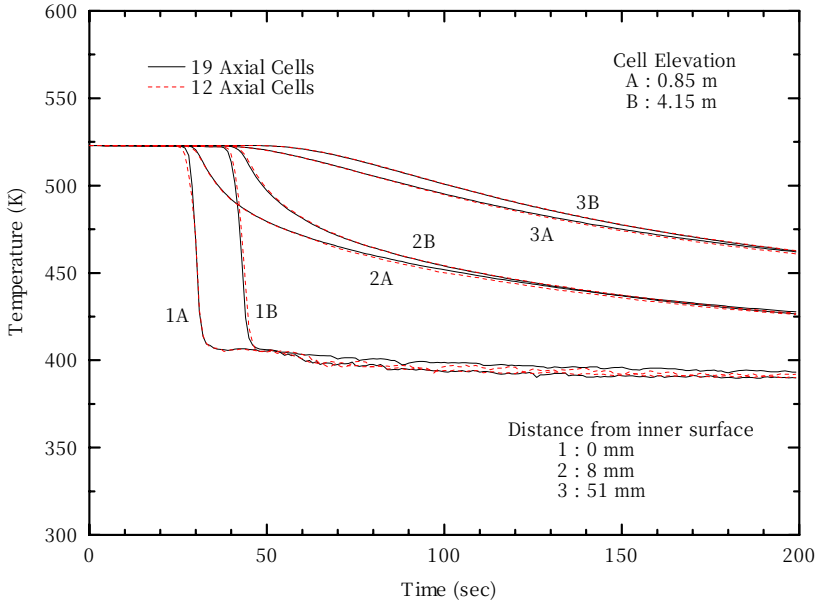

Figure 9 Comparisons of Temperature Histories for Different Axial Cell Numbers

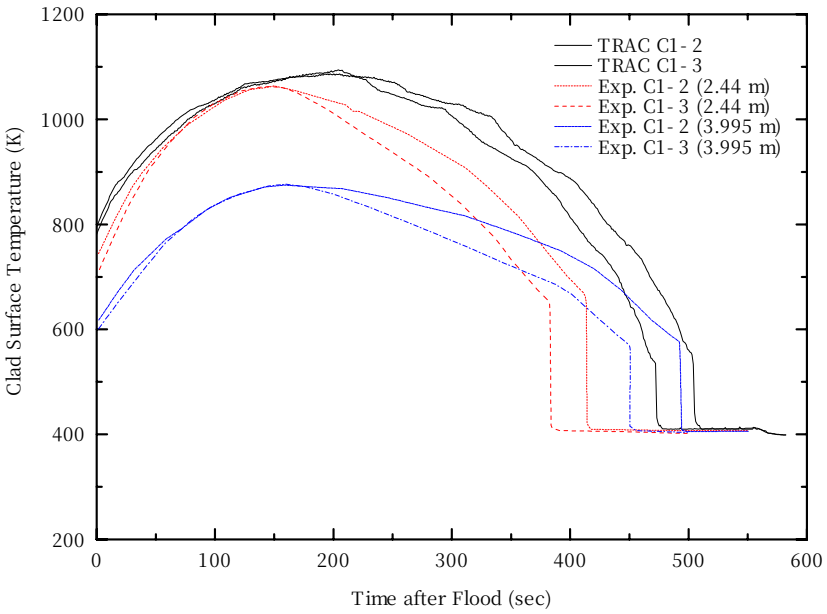

Figure 10 Comparisons of Clad Surface Temperatures

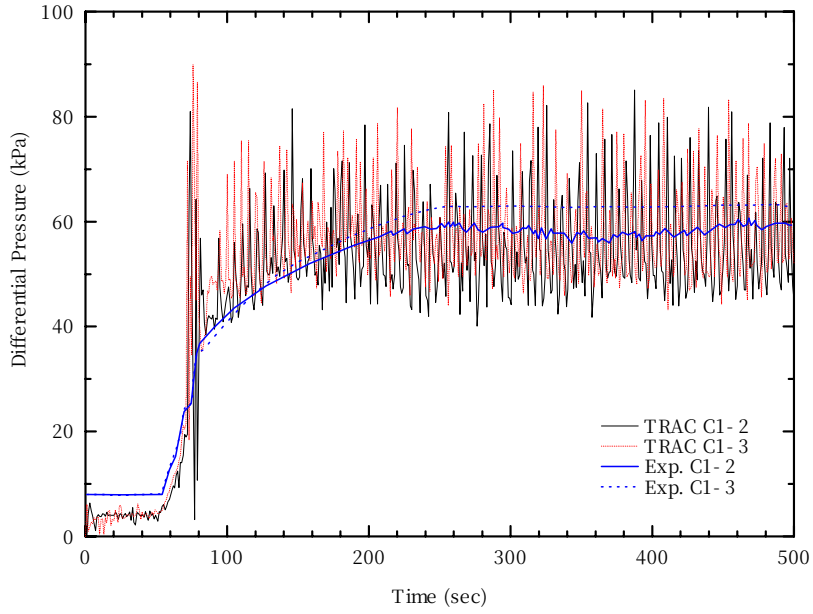

Figure 11 Comparison of Differential Pressure at Downcomer

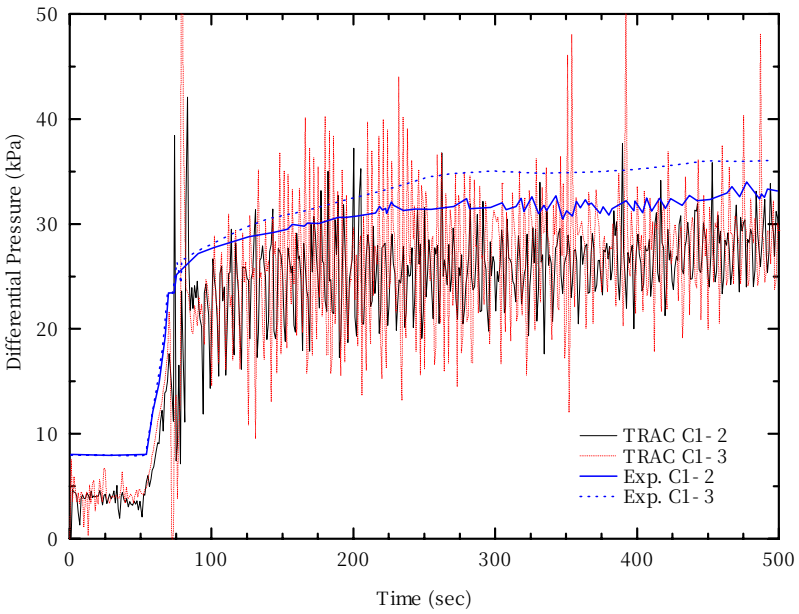

Figure 12 Comparison of Differential Pressure at Core

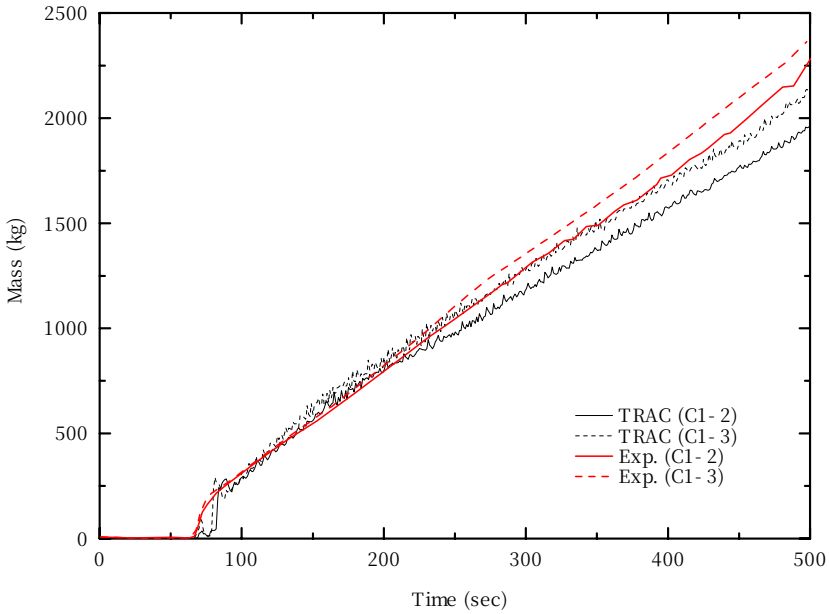

Figure 13 Comparison of the Water Mass Collected in Core